Originally posted 5 July 2012; corrected 10 July 2012

www.sciencemag.org/cgi/content/full/336/6090/88/DC1

Supplementary Materials for

A Single Promoter Inversion Switches *Photorhabdus* Between Pathogenic and Mutualistic States

Vishal S. Somvanshi, Rudolph E. Sloup, Jason M. Crawford, Alexander R. Martin, Anthony J. Heidt, Kwi-suk Kim, Jon Clardy, Todd A. Ciche*

*To whom correspondence should be addressed. E-mail: ciche@msu.edu

Published 6 July 2012, *Science* **337**, 88 (2012)
DOI: 10.1126/science.1216641

This PDF file includes:

Revised 10 July 2012: Author changes were received 25 June. Antibiotic tolerance methods were added, and other minor changes were made.

Materials and Methods

Strains and culture conditions**.**

The nematode and bacterial strains and plasmids used in the study are listed in Table S3 (below). Chemicals were obtained from Sigma-Aldrich (St. Louis, MO) unless otherwise indicated. *Escherichia coli* was grown at 37°C in lysogeny broth (LB) modified to contain 5 g/liter NaCl (Becton, Dickinson and Co., Franklin Lakes, NJ. Agar (1.5%), ampicillin (50 μg/ml), chloramphenicol (125 μg/ml), gentamicin (5 μg/ml) and diaminopimelic acid (300 μg/ml) were added when required. *Photorhabdus* spp. were grown at 28°C in LB supplemented with 1 g/liter sodium pyruvate (LBP). Agar (1.5%), chloramphenicol (15 μg/ml), gentamicin (0.75 or 5 μg/ml), streptomycin (40 μg/ml), ampicillin (100 μg/ml) and kanamycin (3.75 μg/ml) were added when required.

Nucleic acid purification and molecular biology techniques**.**

Standard molecular techniques were performed as described previously (*31*). Bacterial genomic DNA was purified from a 3-ml culture of *Photorhabdus* grown in Grace's insect cell culture medium (Invitrogen; Carlsbad, CA) using DNAeasy tissue kit (Qiagen; Alameda, CA). Plasmid DNA was purified using Qiagen Plasmid Mini or Maxi preps. DNA was extracted following agarose gel electrophoresis using Zymoclean Gel DNA Recovery Kit (Zymo Research Corporation, Irvine, CA). Restriction endonucleases and T4 ligase were used per the manufacturer's instructions unless otherwise indicated (Invitrogen or New England Biolabs; Ipswich, MA).

Nematode propagation**.**

Axenic IJs of the inbred *H. bacteriophora* strain M31e nematodes were harvested from lawns of the GFP-labeled **tr**a**n**smission mutant (TRN)16, which is completely defective in IJ nematode colonization on NA-corn oil (Nutrient broth 8 g, agar 15 g, corn oil [Mazola] 12 mL/per liter) added to one side of 100 mm diameter split Petri dishes for 10-14 d (*10*). Sterile Ringer's solution (100 mM NaCl, 1.8 mM KCl, 2 mM $CaCl_2$, 1 mM $MgCl_2$, and 5 mM HEPES pH 6.9) or saline (0.85% NaCl) was added to the empty half of the plate to trap the dispersing IJs which were harvested, surface sterilized by incubating the IJs in 2% Clorox Ultra (0.12 % sodium hypochlorite, Clorox Commercial, Oakland, CA) for 5 min, washed 3 times each with 15 ml of Ringer's by centrifugation, and the nematode stocks were stored in 7 ml Ringers containing 100 μg/mL streptomycin, 100 μg/mL ampicillin, 30 μg/mL kanamycin, and 10 μg/mL gentamicin to maintain the sterility.

Nematode Pulse-chase and adherence assays**.**

GFP-labeled bacteria transiently present in nematode intestines were replaced by unlabeled or dsRED-labeled bacteria by pulse chase experiments so that only persistent GFP-labeled bacteria were present (*11*). Axenic IJ nematodes were added to GFP-labeled bacterial lawns on NA+chol, incubated at 28°C for 38-42 hours (pulse), then transferred to plates containing dsRed or unlabeled *Photorhabdus* and incubated for 4 hours (chase) to allow the nematodes to clear transient GFP-labeled symbionts from their intestine. The nematodes were assayed for the presence of adherent and persistent bacterial strains using an epifluorescence compound microscope (DM5000, Leica Microsystems, Wetzlar, Germany) equipped with a Spot Pursuit

CCD camera (SPOT Imaging Solutions, Sterling Heights, MI), X-Cite120 Illumination System (EXFO Photonic Solutions Inc., Mississauga, Ontario) *gfpmut3* and dsRed filter sets (Leica).

Detection of M-form small colony variants from maternal nematodes.
Up to 50 IJ nematodes were pulsed on NC1Tn7GFP or TTO1Tn7GFP lawns for 38-42 hours as described above, and chased for 4 hours on NC1Tn7dsRed or TTO1, respectively. These nematodes were washed once in Ringer's, and 20-30 nematodes were grinded by a motorized tissue grinder (Kontes Glass Co; Vineland, NJ). The ground sample was diluted and spread on LBP agar plates and incubated at 28°C for 72 hours to observe the colony morphology of the adherent and the transient cells. M-form colonies were small, translucent, and developed sectors of the P form after 3 days. P-form cells were opaque, pigmented, convex with smooth margins and a regular appearance.

Enumeration of P and M forms inside nematodes, insects and aged colonies.
Approximately 50 axenic IJ nematodes were inoculated on lawns of TT01GFP and *madswitch*GFP (*madA::gfpmut3**) strains, which reports the switch in the ON orientation and is described below. At 24, 38 and 56 h after inoculation, 10 nematodes were picked from each lawn, washed in Ringer's solution, homogenized, plated on LBP agar plates and incubated at 28°C for 72 hours. The GFP expressing adherent M-form and the non-GFP transient P-form cells were scored. To quantify the M and P forms outside nematodes, cells from the lawn were resuspended in LBP broth and plated. The experiment was repeated 2 independent times in triplicates, and the data were analyzed by two-way ANOVA using GraphPad Prism (GraphPad Software, Inc., La Jolla, CA). For quantification of bacterial forms inside the insects, approximately 10 P-form TT01 and *madswitchGFP* cells were injected into *Galleria mellonella* larva (Grubco Inc., Fairfield, OH). Sterile LBP broth served as negative control. At days 1, 2, 3, 4, and 8, individual dead insects were surface sterilized, and the bacteria were collected by inserting a sterile needle into the insect cadavers and suspending the bacteria in LBP. The M- and P-form colonies were counted at 72 hours after plating. The experiment was repeated at least 3 independent times and statistically analyzed by one-way ANOVA followed by Tukey's multiple-comparison test using GraphPad Prism. Formation of M-form bacteria on aging plates was determined by aging freshly thawed bacterial strains on 100- × 15-mm Petri plates, each containing 25 ml of LBP agar medium. The plates aged on lab benches at room temperature for up to 60 days. At 15, 30, 45 and 60 days, the cells were resuspended in LBP, plated and enumerated using plate count method.

Allelic exchange.
Recombineering (i.e., lambda RED facilitated homologous recombination) (*32*) was developed to facilitate genetic manipulations of *Photorhabdus* (Fig. S6). Recombineering involves transient expression of highly efficient *E. coli* λ- red recombination genes *exo*, *bet* and *gam* to achieve homologous recombination. A mutant allele (e.g., deletion) was constructed by fusing >600 bp flanking the gene to a selectable gentamicin resistance (Gm^R) marker flanked by Flippase (Flp) recombinase target (FRT) sites as described (*33*) using High Fidelity Platinum Taq DNA Polymerase (Invitrogen). The primers used are listed in Table S4. The flanking sequences and antibiotic resistance cassette were first amplified separately and then combined and fused by strand overlap PCR. The cycling conditions for the first PCR were: 95°C for 2 min, followed by 30 cycles of 94°C for 30 s, 56°C for 30 s, and 68°C for 1 min, and a final extension at 68°C for

10 min. The flanking products were then fused to FRT-Gm^R-FRT cassette amplified from pPS856 (*33*) by fusion PCR, comprising an initial denaturation at 94°C for 2 min, 3 primer-less cycles of 94°C for 30 s, 55°C for 30 s and 68°C for 1 min (3rd cycle was paused at 68°C to add 5'up and 3'dn primers), 25 cycles of 94°C for 30 s, 56°C for 30 s, and 68°C for 5 min, and final extension at 68°C for 10 min. The mutant allele PCR fragment was extracted from the agarose gel, and quantified by Nanodrop Spectrophotometer (Thermo Scientific, Wilmington, DE) and agarose gel electrophoresis.

To achieve recombineering, 1-2 μg of plasmid pSIM5 (*6*) carrying the λ-red recombination genes was transformed into TTO1, and transformants were selected by chloramphenicol resistance. Prior to preparation of electro-competent cells, λ-red genes were induced by exposing TTO1 + pSIM5 cell culture (OD_{600} = 0.2-0.3) to 42ºC for 15 min (Fig S6). Then, 4-5 μg of the mutant allele (constructed as above) was transformed into the cells by electroporation and recombinants were selected by gentamicin resistance (Gm^R, 5 μg/ml gentamicin) plates. Usually 10-100 Gm^R recombinant colonies were obtained. Selection for the desired recombinant types was determined using three PCR assays using primers listed in Table S4. Once validated, the Gm^R marker was removed by site specific recombinase Flp, expressed from plasmid pCP20 (*35*) or pFLP2 (*36*) transformed into the Gm^R recombinants. Expression of Flp recombinase was induced by heat shock at 42ºC for 15 min, and the desired recombinant was verified by PCR.

Genetically locking the *madswitch* invertible promoter in OFF and ON orientations.

madswitch was locked into ON and OFF orientations in the P form using recombineering (Fig S7). To lock the *madswitch* OFF, a mutant allele was constructed by fusion PCR deleting *madR* and inverted repeat left (IRL) in OFF oriented P-form cells. DNA upstream and downstream of the deletion was obtained by PCR using primers Lock-5'Up, Lock-5'Dn-Gm, Lock P-3'Up-Gm and Lock-3'Dn primers listed in Table S4 using P-form (wt) genomic DNA template. To lock the *madswitch* ON, a mutant allele was constructed using the same upstream primers and using LockM-3'Up-Gm and Lock-3'Dn primers to amplify the *madswitch* ON from M-form DNA. The PCR amplified DNA captured the *madswitch* promoter in OFF or ON orientations respectively, and contained a 304-bp or 209-bp sequence containing rightward inverted repeat (IRR) upstream of *madA,* respectively. These PCR products were fused to the FRT-Gm^R-FRT by fusion PCR as described above**.** These mutant alleles were recombined into TTO1 chromosome resulting in *madswitch* locked in OFF or ON orientations, and deletion of *madR* recombinase and the left inverted repeat (IRL) to disrupt *madswitch* inversion. The mutants were named locked P form (L/P form) or locked M form (L/M form), respectively.

Complementation.

We previously complemented a *madJ* mutant by expressing *madIJK* or *madA-K* on a plasmid in *trans*, which resulted in the partial restoration of maternal adhesion phenotype to the *madJ* transposon mutant (*11*)**.** However, these experiments were difficult because of poor plasmid maintenance in *Photorhabdus.* We inserted a *gfp* reporter into several plasmids (e.g., pBBR1MCS1 and pARA3) and observed plasmid loss in ~40% of the cells after overnight growth with antibiotic selection. Thus, complementation experiments to restore the switching to the M-form phenotype in mutants such as *madJ* were problematic.

Phenotypic characterization of strains.

Actively growing overnight cultures of enriched P-and M-form cells, and L/P-and L/M-form strains from freshly thawed freezer stocks were used for the phenotypic assays.

Growth rate was determined by first preparing overnight starter cultures in LBP broth at 28°C. These cultures were diluted to $O.D._{600}$ = 0.01 in LBP; 200 µl of the diluted culture ($O.D._{600}$=0.01) was inoculated in a 96-well polystyrene plate (Corning Incorporated, Corning, NY) in triplicates and the plate was sealed with parafilm to prevent drying. The plate was incubated at 28°C in a microplate reader (SpectraMax M5, Molecular Devices, Sunnyvale, CA) equipped with analysis software SoftMax Pro (Molecular Devices), programmed to take $O.D._{600}$ readings every 30 min until the growth curves reached a plateau. The experiment was repeated twice. To determine the doubling time, we picked 4- to 15-hour time points representing exponential growth phase (Fig. S8). The specific growth rate/hour (µ) was calculated by using the formula;

Specific growth rate (µ)= 0.6931/doubling time (hours)

*Competition assays***.** Overnight cultures of L/P- and L/M-form cells were diluted to OD_{600} = 0.1, which corresponds to 4-7 million CFUs/ml for P form and 20-50 million CFU/ml for M form. Approximately 100 cells of both P and M forms were competed against each other in a test tube in LBP broth by growing them together for 24 hours at 28°C. The initial and final counts were done for competition tubes by serial diluting and plating on LBP agar plates. The competition index was calculated using the following formula:

Competition Index = (Final no. of P-form cells/Final no. of M-form cells)/(Initial no. of P-form cells/Initial no. of M-form cells)

Cell shape, size and volume were determined by phase-contrast microscopy of L/P- and L/M-form cells in stationary phase in a phase-contrast compound microscope (DM5000, Leica). The images were analyzed using CMEIAS Ver. 1.27 (*37*) operating in UTHSCSA Image Tool Ver. 1.27 (*38*). The approximate volume of the cells was calculated by using the formula derived from summation of volume of a cylinder and a sphere. Volume of cell = $\pi r^2[h+(4/3)(r)]$
where r is radius of cell (= width/2), h is height of cell (= length – width). The data were statistically compared using unpaired Student's *t* test.

Pigmentation of colonies was determined by visual inspection and digital color photography of colonies grown on LBP for 48 hours at 28°.

The production of antibiotic activity was determined by growing *Photorhabdus* on LBP plates for 48 hours. These cultures were then killed by exposing the plates to chloroform fumes for 30 min, followed by air drying for 30 min. On top of each plate of *Photorhabdus* strains, 6 ml of LB with 0.7% agar mixed with 25 µl overnight culture of *Micrococcus luteus* was overlaid.

The production of siderophore activity was determined as described previously (*39*) except that the chrome azural S (CAS) solution was added to LB agar. Siderophore activity was detected as zone of clearing where iron was removed from the blue CAS-Fe(III)-hexadecyltrimethylammonium bromide complex.

Hemolysis activity was determined on sheep blood agar plates, and *bioluminescence* was assayed from 48-hour-old *Photorhabdus* colonies using a NightOWL 980 Moleular Imaging System (Berthold Technologies**,** Oak Ridge, TN) equipped with a WinLight32 software. *Absorption of neutral red* was assayed on MacConkey agar (BD, Franklin Lakes, NJ). *Absorption of eosin and methylene blu*e was assayed on EMB agar (BD). *Congo red absorption* was assayed on LB agar supplemented with 0.01% Congo red. Nutrient agar (BD) supplemented with 0.025% (w/v) bromothymol blue and 0.004% (w/v) triphenyltetrazolium chloride (NBTA) was used to assay the uptake or reduction of these dyes. *Crystal inclusion protein* (Cip) *production* was determined by phase-contrast microscopy of 72 h cultures. *Swimming and swarming motility* was determined on LBP with 0.35% and 0.8% agar supplemented with 0.025% bromothymol blue and 0.004% triphenyltetrazolium chloride (*40*).

Pathogenicity to insects was determined by injecting 10 µl LBP broth containing ca. 100 bacteria behind first forelimbs of the 3rd instar *Galleria mellonella* larvae (GrubCo Inc., Hamilton, Ohio) using a Hamilton syringe with a 28 gauge needle (Hamilton Co; Reno, NV). Sterile LBP was used as a negative control. Following injections, the insects were incubated at 25ºC, and survival was assessed every 24 hours for 6 days. Insect survival data were analyzed using Kaplan-Meier survival curves with Log-rank test to compare the statistical significance using software GraphPad Prism. *P* values of <0.05 were considered statistically significant.

Biofilm production on polystyrene was assessed by incubating 200 µl of the $O.D._{600}$ = 0.01 normalized cultures of L/P and L/M forms at 28°C for 96 hours in parafilm sealed 96-well polystyrene plates (*41*). TTO1 was used as control. Biofilms were stained with crystal violet, and washed twice with water. Then, 200 µl of 33% acetic acid was added to the wells to release the stain and was measured as the absorbance at 590 nm. The experiment was repeated twice with at least 6 replicates in each experiment. Data were statistically compared using one-way ANOVA followed by Tukey's multiple comparison test using GraphPad Prism. *P* values of < 0.05 were considered statistically significant.

Metabolite analysis.
P. luminescens TT01, L/M, and L/P were streaked on LB plates from cell stock and grown at 30°C for 2 days. Single colonies were inoculated into 5 mL of a tryptone/yeast extract medium (2 g tryptone, 5 g yeast extract, and 10 g NaCl per L) and grew overnight at 30°C and 250 rpm. The overnight culture (50 µL) was used to inoculate 5 mL of fresh tryptone/yeast extract medium supplemented with 100 mM L-proline. The cultures were grown at 30°C and 250 rpm for 48 h, and the whole cultures were rigorously extracted with 6 mL of ethyl acetate. The layers were separated by centrifugation, and the top 4 mL of ethyl acetate was transferred to a glass vial, dried, and resuspended in 500 µL methanol for liquid chromatography-mass spectrometry analysis (Agilent 6130). The extracts were analyzed by LC/MS as described previously (*19*) for stilbene and anthraquinone quantification. The organic extracts were separated over a Discovery RP-amide C16 (25 cm × 4.6 mm, 5 µm, Supelco) HPLC column with an acetonitrile:water gradient (1 mL/min): 0-2 min, 10% acetonitrile isocratic; 2-10 min, 10-50% acetonitrile; 10-25 min, 50-75% acetonitrile. Chromatographs were monitored using diode array spectrophotometry and positive and negative ion MS.

Antibiotic tolerance experiments were performed from overnight cultures of L/M and L/P form in LBP broth at 28°C, then diluted 100-fold and 1000-fold in 3 ml LBP, respectively, and grown until the cultures reached 1×10^8 CFU/mL (~7.5 h). Antibiotic was added and every 0.5 hours up to 3 hours a 100µl sample was taken, washed via centrifugation, and plate counts determined. The experiments were performed in triplicate and repeated at least three times. Data were analyzed by unpaired 2-tailed Student's *t* test and *P* values ≤ 0.01 were consider significantly different.

Determination of switching frequency between M and P forms.
The frequency of form switching was determined by the P_0 method. First, the unstable M form was purified by streaking 10-12 isolated M-form colonies (from nematodes isolated as described above) after 24 hours of growth, when M-form colonies are just visible and have less P-form cells than older colonies. The P form was similarly isolated by streaking 10-12 colonies of P-form phenotype. Isolations were repeated three times and then freezer stocks (LBP with 4.5% dimethyl sulfoxide) were made by scraping colonies after 24 hours of growth on LBP. Switching frequencies were determined from M- and P-form cells following 24 hours of growth on LBP plates thawed from freezer stocks. The cells were suspended in LBP, optical density was determined and then the cells were diluted to extinction. After 24 hours, less than half of wells had growth, which were diluted and the generation determined when switching to the other form occurred, which is likely an underestimate since selection was not employed.

*madswitch*GFP reporter and switching assays.
A *madswitch*GFP reporter strain was constructed to report the switching of the *madswitch* in the ON orientation and expression of the *mad* locus at single cell resolution during nematode mutualism, pathogenicity to insects and in culture. A promoter-less *gfpmut3** gene was recombined into the TTO1 chromosome between *madA* and *madB* by recombineering so that normal expression of the *mad* fimbrial locus occurred. The promoter-less *gfpmut3** was amplified from positions 3822 to 4590 of pURR25 using primers Fim-reporter-GFP-Up and Fim-reporter-GFP-Dn (Table S4). The FRT-Gm^R-FRT DNA was amplified from pPS856 using primers Gm-F and Gm-R. Similarly, *madA* and *madB* were amplified from TTO1 genomic DNA template using primers Fim-reporter-5'madA-Up and Dn, and Fim-reporter-3'madB-Up and Dn, respectively, using PCR conditions and reagents described above. The primers Fim-reporter-5'madA-Dn, Fim-reporter-GFP-Dn, and Fim-reporter-3'madB-Up introduced overlapping sequence in respective amplicons to 5' end of *gfpmut3**, and 5' and 3' ends of FRT-Gm-FRT in the respective PCR products. 50 ng of individual PCR products generated above were combined by a fusion PCR to generate "*madA-gfpmut3**-FRT-Gm^R-FRT-*madB"* mutant allele. The fusion PCR cycle comprised of initial denaturation at 94°C for 2 min, 3 primer-less cycles of 94°C for 30 s, 55°C for 30 s and 68°C for 2 min (3rd cycle was paused at 1min of the 68°C extension to add Fim-reporter-5'madA-Up and Fim-reporter-3'madB-Dn primers), 25 cycles of 94°C for 30 s, 55°C for 30 s, and 68°C for 6 min, and final extension at 68°C for 10 min. The fused PCR fragment of 3232 bp was extracted from the agarose gel, and quantified. The remaining steps were same as described above.

Determination of transcriptional start site of *mad* fimbriae genes.
The transcriptional start site of the *mad* fimbriae locus was determined by 5' Rapid Amplification of cDNA Ends (5' RACE) (*42*) using GeneRacer kit with SuperScript III RT and TOPO TA

cloning kit for sequencing (Invitrogen) following the manufacturer's protocol. Total RNA was isolated from enriched M-form colonies by using Trizol reagent (Sigma). The RNA was treated with DNaseI (Roche) and de-phosphorylated by calf intestinal phosphate (CIP) to obtain capped mRNA. The capped mRNA was de-capped by treating it with tobacco acid phosphatase (TAP). Subsequently, the RNA-oligo was ligated to the 5' de-capped mRNA transcript using T4 RNA ligase, and reverse transcribed using Superscript III RT and the GeneRacer OligodT primer to create RACE ready first strand cDNA with known priming sites at 5' end. The first strand cDNA synthesised as above was amplified using gene specific reverse primer RACE_*madA* (Table S4) and GeneRacer 5' primer. Additional PCR was performed using nested primers (Table S4), and the product was gel purified and cloned into pCR4-TOPO vector and sequenced at Genomics Core, Research Technology Support Facility at MSU to determine the transcriptional start site for *mad* fimbrial locus. The procedure was independently repeated two different times.

Microarray experiment and quantitative PCR.

Two-color microarray experiments were performed to determine the differences in gene expression between P and M form using *Photorhabdus luminescens* subsp *laumondii* TTO1 3 × 20k microarray (MYcroarray.com, Ann Arbor, MI). RNA was extracted from mid-exponential phase bacterial cultures using Qiagen RNeasy Protect Bacteria Mini Kit (Qiagen Inc., Valencia CA) following the manufacturer's instructions, with an additional step of on-column DNAseI treatment. RNA yield and quality was determined by Agilent 2100 Bioanalyzer (Agilent Technologies, Santa Clara, CA). The RNA labeling and hybridizations were performed at Genomics Core, Research Technology Support Facility, Michigan State University. Reverse transcription of the total RNA population was done to make aminoallyl cDNA followed by attachment of the fluorescent dye using the Fairplay III Microarray Labeling Kit (Agilent Technologies). Hybridization of the labeled cDNA was carried out using Agilent gene expression hybridization and wash reagents and the slides scanned on an Agilent G2505B array scanner. Intensity data were generated by using the GenePix 3.0 software (Molecular Devices, Sunnyvale, CA) and the resulting files analyzed in the GeneSpring 11.0 software (Agilent Technologies, Santa Clara, CA). All arrays were subjected to Lowess normalization. The array features which had intensities in the lower 20th percentile in all channels and all arrays features were filtered out. A *t*-test (against zero) was performed for the triplicate arrays to determine the significantly up (≥2 fold) and down regulated (≤0.5 fold) genes at $P \leq 0.05$. The gene expression ratio was calculated as M/P (fold change in M-form/fold change in P form).

Quantitative reverse transcriptase PCR was used to validate the gene expression results obtained from microarray experiment, 2.5 μg RNA extracted as above was reverse transcribed with Superscript III Reverse Transcriptase (Invitrogen). The primers for genes *madA*, *madK* and *spoT* (Table S4) were designed using Primer3 software (http://frodo.wi.mit.edu/primer3). Quantitative PCR was performed using SYBR green PCR mix reagent (Applied Biosystems, Foster City, CA) and primers in a GeneAmp PCR System 9700 thermocycler (Applied Biosystems). The level of target gene expression was calculated as $2 \exp[-(\Delta\text{M form} - \Delta\text{P form})]$, where ΔM form and ΔP form are the differences in cycle threshold (C_t) for target and reference genes. Standard curves were drawn for all studied genes, and PCR efficiency of those genes were compared with the reference gene to make sure that the $\Delta\Delta C_t$ method is appropriate to calculate their fold expression (Applied Biosystems). To minimize mRNA quantification errors and genomic DNA contamination biases, and to correct for inter-sample variations, we used the *recA* gene as

internal control, and the relative expression ratio was based on the expression of a target gene relative to that of *recA* mRNA as noted above.

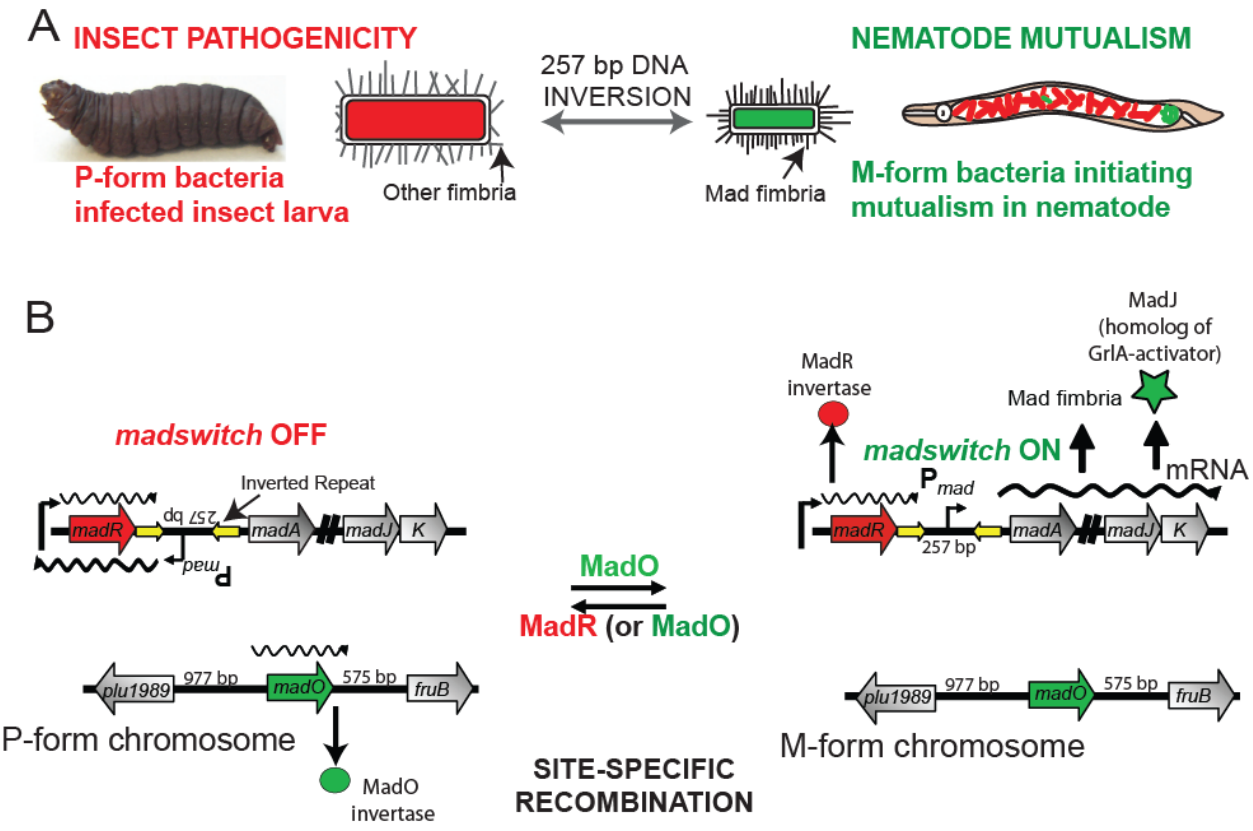

Figure S1. Summary and model for *Photorhabdus* switching between pathogenic and mutualistic lifestyles.
(A) Left. The P-form grows exponentially and produces insecticidal toxins and other virulence factors to function as a highly virulent insect pathogen. P-form bacteria are large cells and produce toxins and secondary metabolites such as antibiotics to preserve the insect cadaver and yellow-red anthraquinone pigments that give infected insects a brick red appearance). A large P-form cell is colored red. Right. Small M-form cells selectively adhere to the posterior nematode intestine and thereby initiate mutualism. The more numerous P-form cells are only transiently present in the nematode intestine. The M form lacks pathogenicity and most phenotypic characteristics of the P form. **(B)** Model of the mechanism by which promoter inversion regulates lifestyle switching. Left**.** The P form has the *madswitch* oriented OFF and thereby does not express the *mad* genes. Expression of the MadR invertase may be inhibited due to counter transcript driven attenuation from the *mad* promoter. Expression of the MadO invertase is required to flip the *madswitch* to the ON orientation. Right. In the *madswitch* ON orientation the cells are the M form and express Mad fimbria essential for adhesion and MadJ required for the switch to the M form. The MadR is required for efficient switching to the *madswitch* OFF and P form in the infective juvenile offspring thereby arming the nematodes for insect infection.

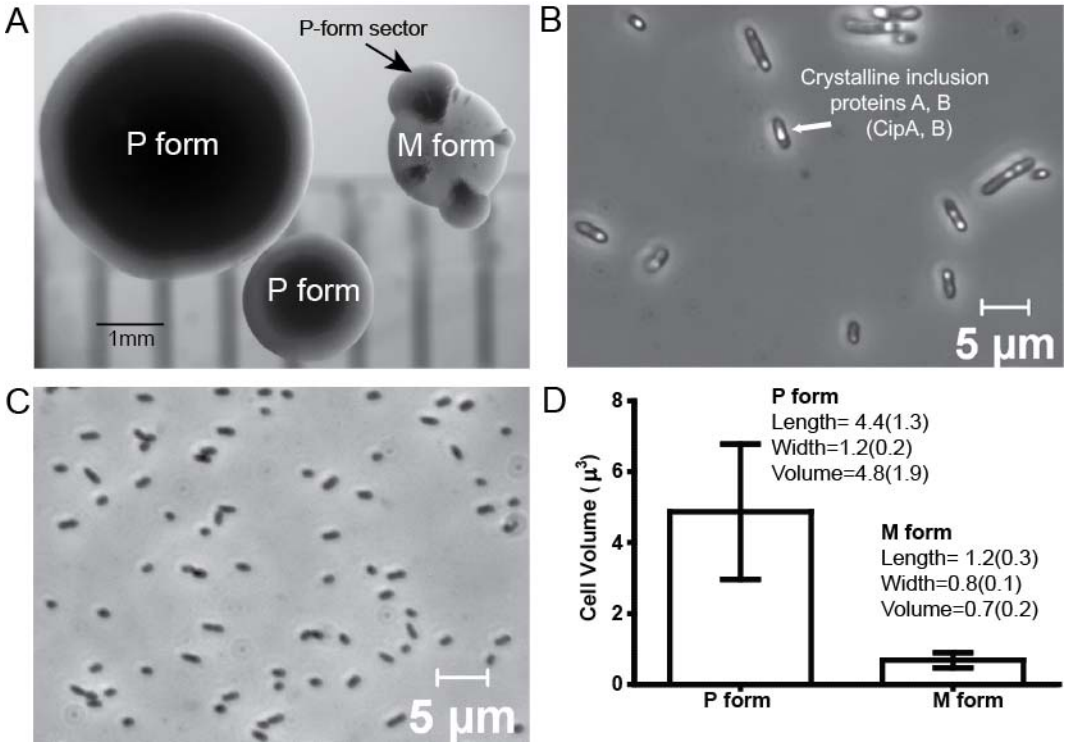

Figure S2. Colony and cell morphology of P and M form.
(**A)** Representative colonies of P form and M form at 72 hours on LBP plates, A sector of P-form cells irrupting from an M-form isolated colony is indicated. A small P-form colony that is opaque and lacking sectors is also indicated. (**B)** P-form cells are larger and show presence of crystalline inclusion proteins CipA and CipB required for nematode reproduction, and (**C)** M-form cells are smaller with no visible inclusions. (**D) T**he volume of P-form cells (n = 46) is up to 9 times greater than M-form (n = 205) cells. Unpaired Student's t-test, P<0.0001, Numbers in parentheses shows standard deviation.

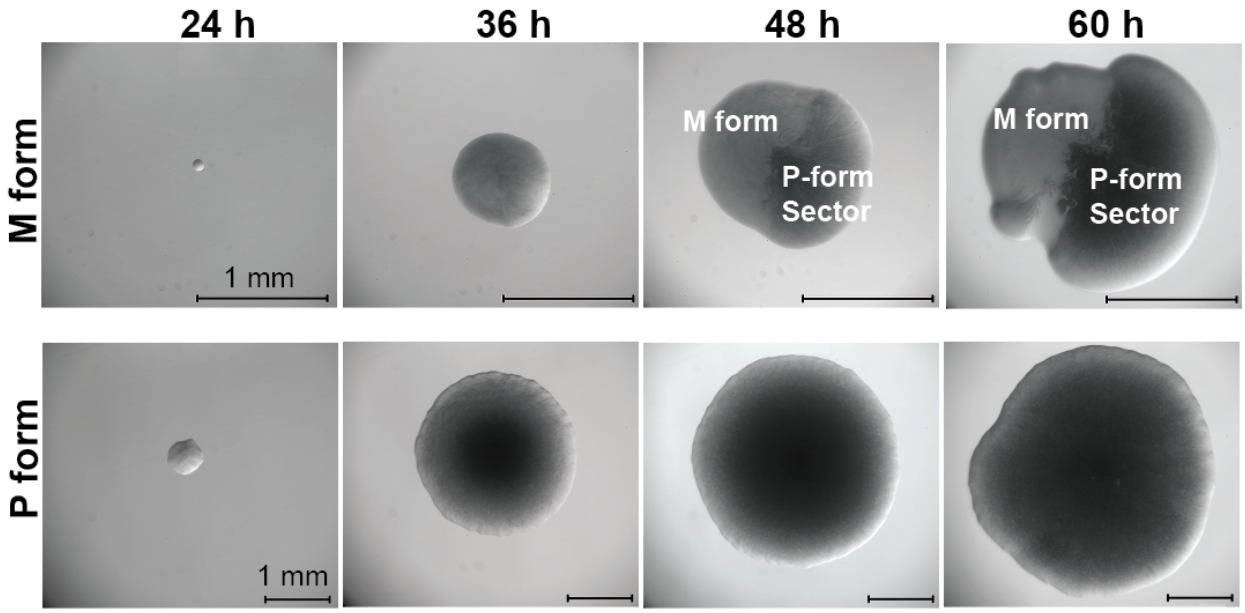

Figure S3. Development of M-form and P-form colonies.
M form develop small colonies resembling small colony variants (SCVs). Sectors of the P form were visible after 36 h and became predominant after 48 h. At 60 h, the M-form colony becomes uneven and sectored with opaque P-form cells (darker in the image). The P form dominates to the extent that an M-form colony switches to a P-form phenotype. P form makes opaque round colonies without any visible sectoring. Scale bar = 1 mm.

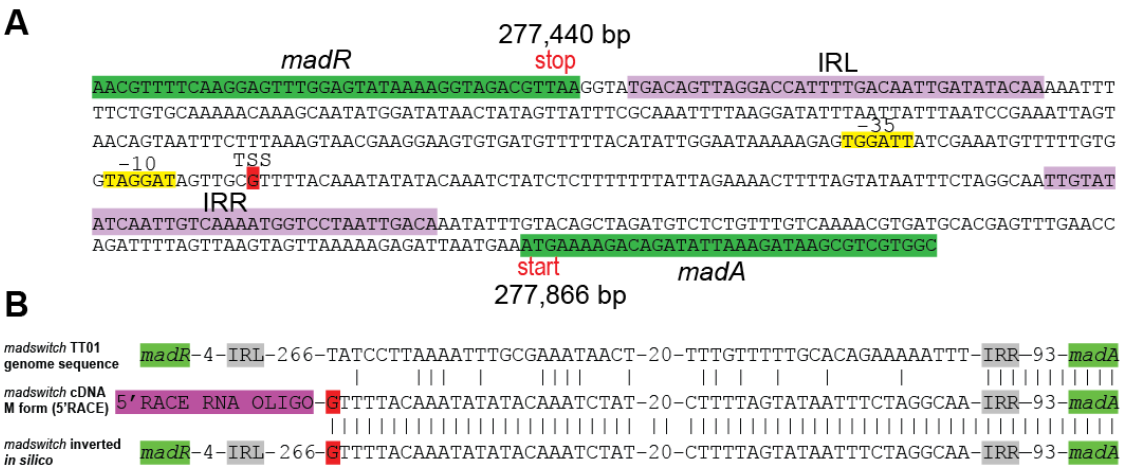

Figure S4. Transcription of *mad* is initiated from 257 bp promoter inversion of the *madswitch* from the P-form and TT01 genome sequence.
(**A)** *madswitch* in the ON orientation (i.e., DNA inverted between inverted repeats IRL and IRR, purple), stop site of *madR*, -35 and -10 sites (yellow), transcriptional start site for *mad* (red). (**B)** DNA alignment of the invertible *madswitch* promoter from P form (oriented OFF), inverted (i.e., reverse compliment of sequence between IRL and IRR) and sequence data from the DNA product of 5' rapid amplification of cDNA ends (RACE) from M form ($n = 2$). Transcriptional start site (red) is from *madswitch* promoter inverted ON in the M form relative to the OFF orientation of the P form.

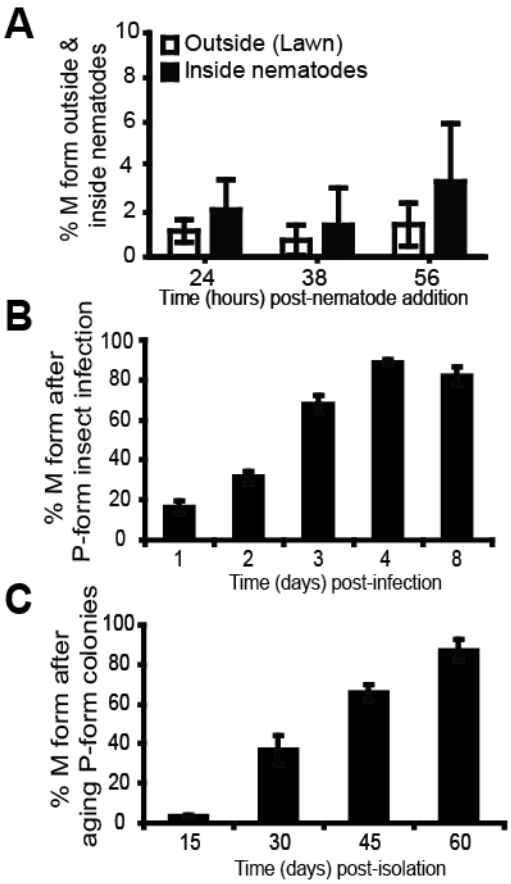

Figure S5. M-formation by the P form under different conditions.
(**A)** M formation is similar outside and inside host nematodes indicating little or no induction of switching in the nematode intestine. (**B)** During P form infection of insects M formation occurs sooner with up to 90% of *Photorhabdus* cells being the M form 4 days after infection. (**C)** M formation occurred later upon aging P-form colonies on LBP agar, with the M form prevalent after 45 days. Error bars represent standard deviation.

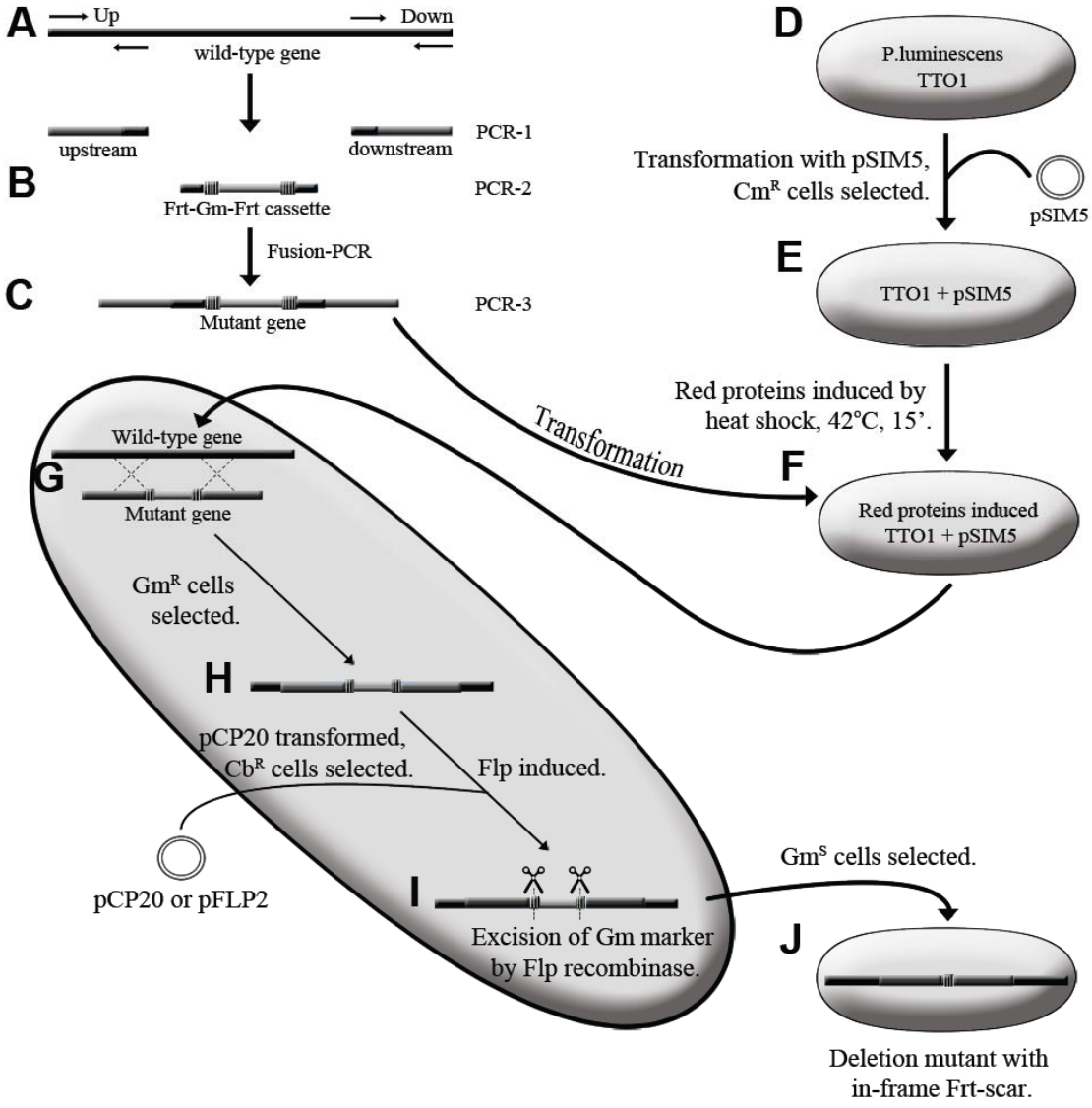

Figure S6. Allelic exchange methodology in *Photorhabdus*.
Recombineering was developed for the efficient manipulation of the *Photorhabdus* genome. Schematic representation to construct an in-frame gene deletion in *Photorhabdus* is shown. (**A)** Up (5') and down (3') ends of wild-type genes were amplified using PCR. (**B)** FRT-Gm^R-FRT cassette was PCR amplified from plasmid pPS856. (**C)** The fragments made during A and B were fused by fusion PCR to create a mutant allele having >600-bp homology to the wild-type gene. (**D-E)** Wild-type TTO1 was transformed with pSIM5 carrying λ-Red genes into the bacteria. (**F)** The λ-Red genes were induced by heat shock, and the mutant allele created by PCR was transformed into the bacteria. (**G-H)** Mutant allele recombines in the wild type chromosome resulting in Gentamicin resistance. **(I)** Flp recombinase is transiently expressed by transforming pCP20 or pFLP2 into the Gm^R cells, which excises Gm^R marker and (**J)** results in the creation of a deletion mutant with an in-frame FRT scar.

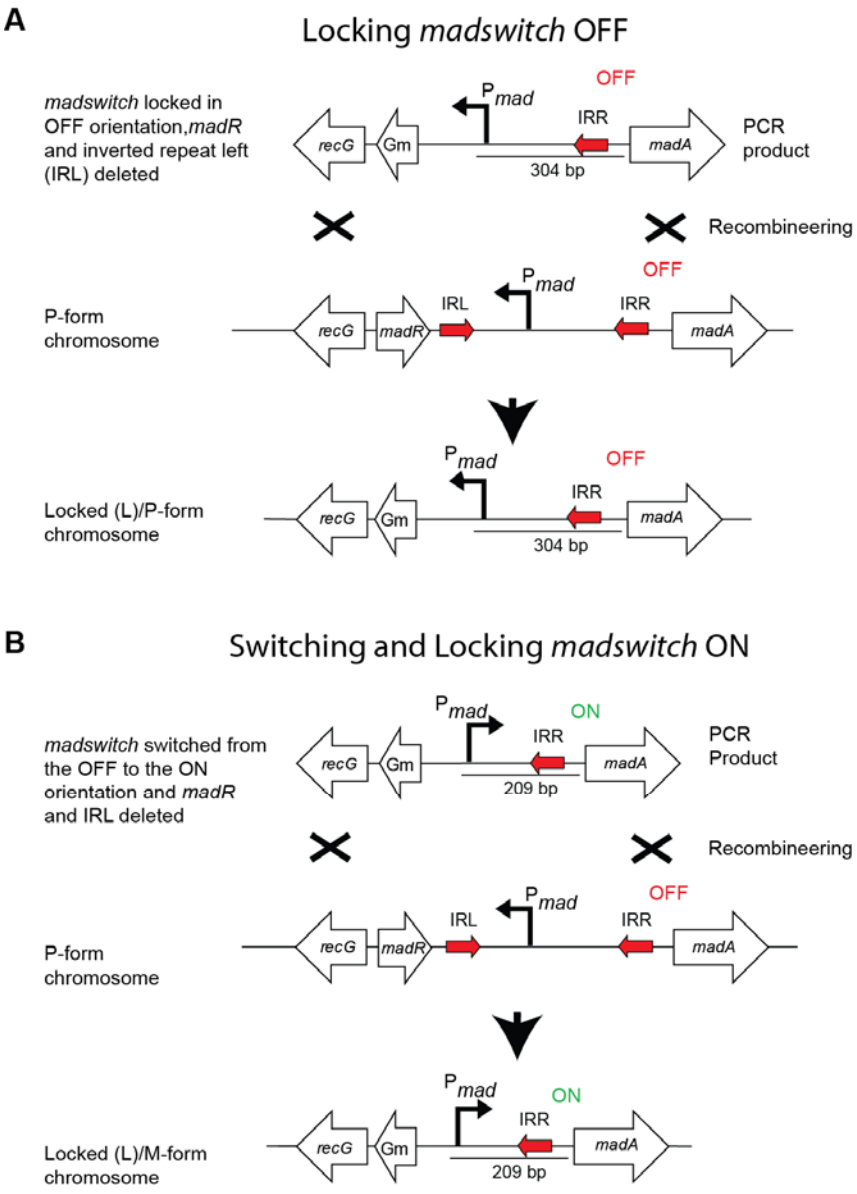

Figure S7. Diagrammatic representation of locking the *madswitch* in OFF and ON orientations.

madswitch was locked ON or OFF in a wild-type P-form background by recombineering. (**A)** To lock the *madswitch* OFF, a mutant allele was constructed by fusion PCR by fusing separately amplified *recG*, FRT-Gm-FRT cassette, and *madswitch* in OFF orientation from purified P-form cells. This mutant allele was recombined into TTO1 chromosome, resulting in *madswitch* locked in OFF orientation and the deletion of *madR* and the left inverted repeat. (**B)** The *madswitch* was locked in ON orientation similarly, except that to construct the mutant allele the *madswitch* was amplified in ON orientation from a purified M-form culture and recombined into the P-form chromosome resulting in an inverted and locked *madswitch* in the ON orientation.

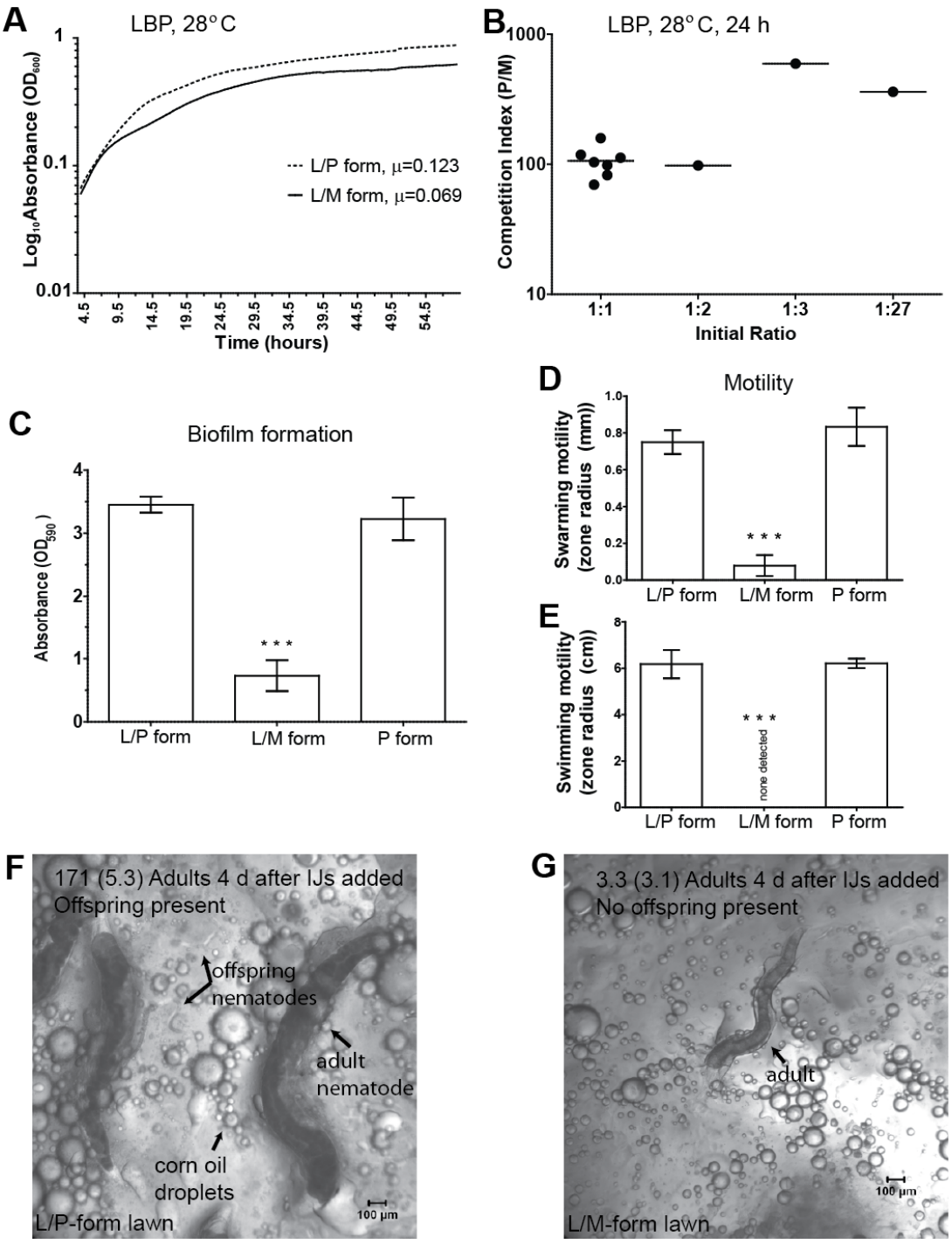

Figure S8. Phenotypic differences in characteristics of P and M forms.
(A) the P form had a higher specific growth rate (μ) compared with M form. (**B)** the P form was more competitive than M form. (**C)** M form developed less biofilm on polystyrene, and (**D-E)** exhibited much less swarming and swimming motility compared with the P form. Error bars show the standard deviation. (**F)** IJ nematodes exit diapause and develop to adults that reproduce on L/P-form. (**G)** few nematodes exit IJ diapause and reproduce on L/M form.

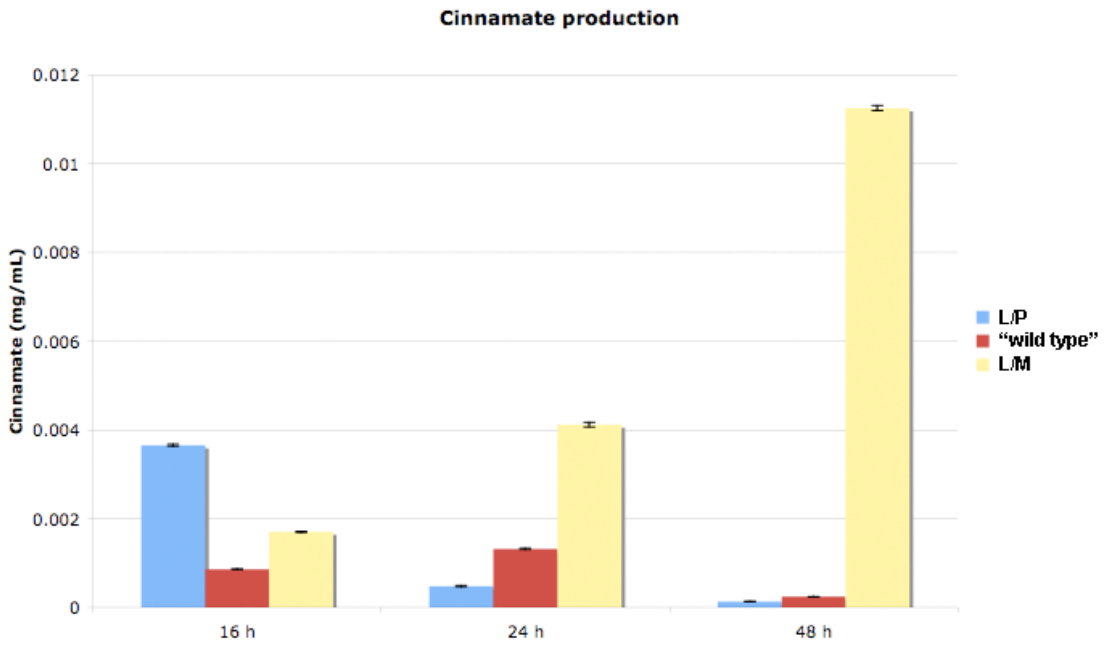

Figure S9. Cinnamate production.
The L/P form initially (16 hours) produced greater cinnamate than "wild type" (P form) and L/M form (n = 3). Later (24 hours and 48 hours), the L/M form produced much greater amounts of cinnamate accumulate than L/P form or "wild type." Cinnamate is converted to stilbene antibiotics by "wild type" and by L/P form. Dramatically reduced stilbene production by the L/M form and less cinnamate degradation may cause its accumulation at 48 hours.

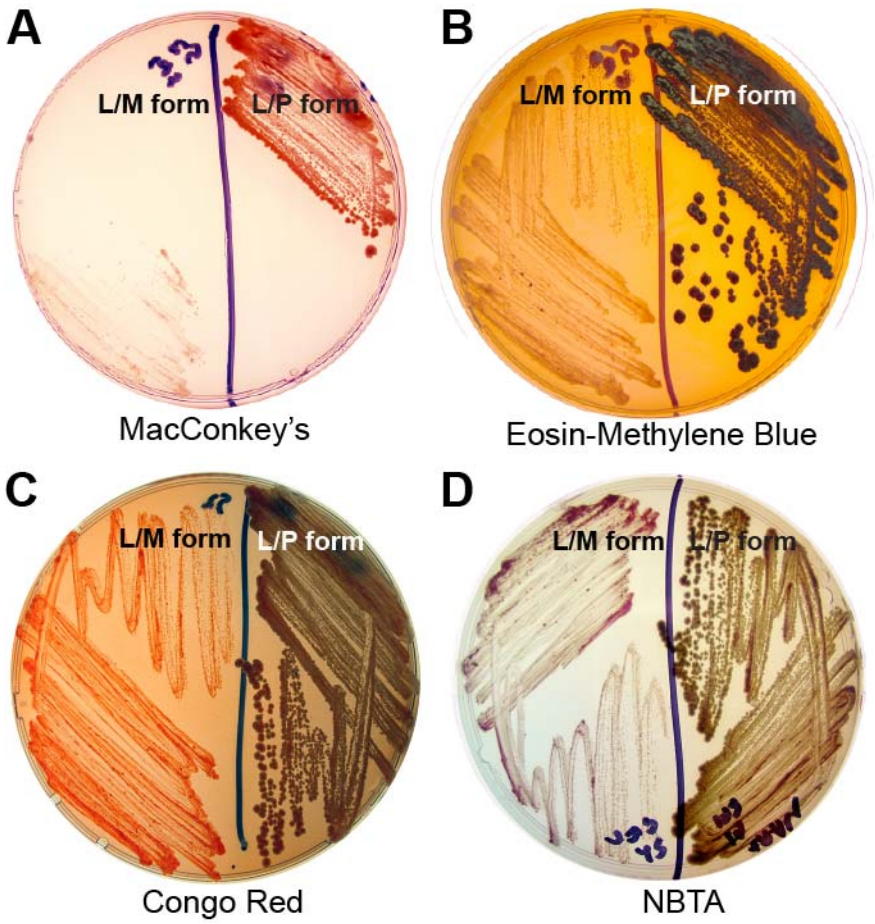

Figure S10. Dye absorption of P- and M-form.
(A) M form ferments less lactose to acid, (**B)** absorbs less methylene blue and (**C)** Congo red and (**D)** reduces less tetrazolium chloride dyes than the P form.

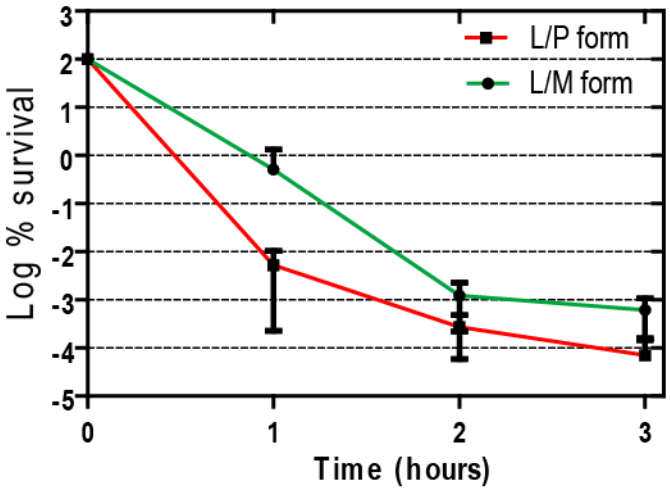

Figure S11. Differential tolerance of the P- and M-form cells to 75 µg/ml streptomycin aminoglycoside antibiotic.

The proportion of L/M-form cells (6.1×10^{-4}) surviving 3-h exposure to streptomycin is 8.7-fold greater ($n = 4$, $P = 0.01$, two-tailed Student's t test) than L/P-form cells (7.0×10^{-5}).

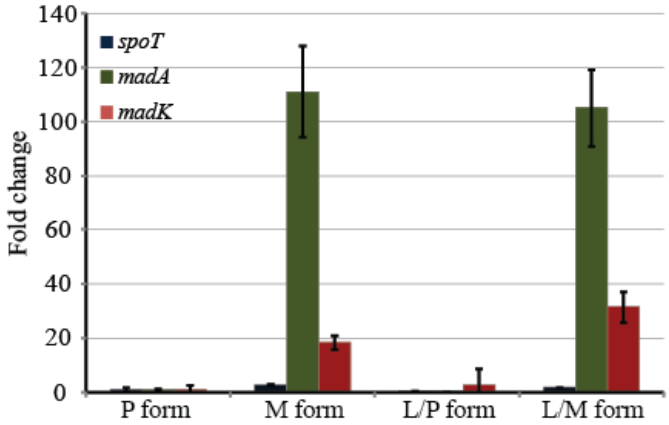

Fig. S12. Quantitative RT-PCR.
Expression of *madA* was elevated approximately 100-fold in the M-form and L/M-form cells than the P-form cells. *madK*, the last gene of the *mad* operon was also up-regulated, but to a lesser extent in the M-form cells than the P-form cells. *spoT,* whose expression was potentially inhibited by counter-transcript–driven attenuation by *madK* expression, was not reduced in the M-forms, which indicated that expression of *spoT* is not inhibited in the M-form. Error bars show standard deviation.

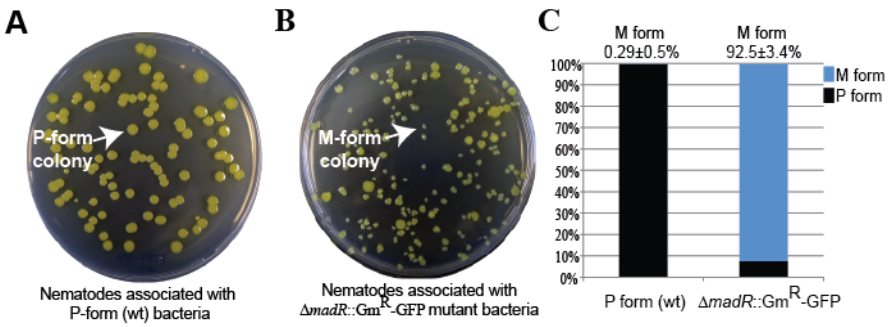

Fig. S13. Increased proportion of M form in fully colonized IJ nematodes associated with Δ*madR* versus P form.

(A) Colonies grew as the P-form from fully colonized IJ nematodes (i.e., after >7-day incubation in saline) associated with the P-form (wt). (**B)** In contrast, colonies grew mostly as the M form after isolation from IJ nematodes associated with the Δ*madR*::Gm^R-GFP. (**C)** the M form is ca. 300 times more prevalent in fully colonized IJs associated with Δ*madR*::Gm^R-GFP than P-form (wt) suggesting that MadR functions in switching from the M-form to the P-form by cells inside the IJ intestine.

Table S1. Comparative transcriptomics analysis of locked M form vs. locked P form; LPB broth, 28 °C, mid-exponential phase. Notable differentially expressed genes out of 265 up-regulated genes (≥ 2-fold, $P \leq 0.05$) and 251 down-regulated genes (≤ 0.5, $P \leq 0.05$).

Gene	Name	Locus tag	Ratio M/P	*P*-value
cse3	CRISPR-associated Cse3 family protein	plu0750	69	0.038
plu1967	PRK15240/Ail_Lom/OmpX unknown outer membrane protein, NOTE: related plu2481 down regulated (see below).	plu1967	43	0.019
madA	major subunit of Mad fimbriae	plu0261	38	0.013
plu3563	Anthranilate/para-aminobenzoic acid synthase	plu3563	26	0.013
plu0826	Rhs_VgrG; possibly Type VI secretion related	plu0826	23	0.023
plu0462	Rhs_VgrG; possibly Type VI secretion related	plu0462	18	0.017
plu2293	Type VI secretion related	plu2293	9.2	0.023
ispH	4-hydroxy-3-methylbut-2-enyl diphosphate reductase, also known as lytB penicillin tolerance protein	plu0594	8.3	0.010
lrhA	Transcriptional regulator LrhA (HexA)	plu3090	4.4	0.011
madJ	DUF1401, GrlA/CaiF-like transcriptional activator	plu0270	4.2	0.036
cipA	crystalline inclusion protein A	plu1576	0.0026	0.006
cipB	crystalline inclusion protein B	plu0157	0.0019	0.003
luxB	alkanal monooxygenase beta chain (luciferase)	plu2082	0.33	0.003
prtA	zinc-dependent metalloprotease serralysin-like	plu0655	0.19	0.026
tccC2	Insecticidal toxin complex protein TccC2	plu0960	0.495	0.021
tccC3	Insecticidal toxin complex protein TccC3	plu0967	0.47	0.029
tccB1	Insecticidal toxin complex protein TccB1	plu4168	0.31	0.006
katE	Catalase	plu3068	0.11	0.005
plu2481	PRK15240/Ail_Lom/OmpX unknown outer membrane protein, NOTE: related plu1967 up-regulated (see above).	plu2481	0.23	0.014

Table S2. Genes differentially expressed in the M form relative to the P form with predicted metabolic, cell surface and regulatory function**.**

M/P	Gene	Locus tag	Description	*P*
Metabolic function				
9.4	*fruK*	plu2858	1-phosphofructokinase (fructose 1-phosphate)	0.040
9	*atpD*	plu0040	ATP synthase beta chain	0.024
8.8	*Eda*	plu0178	KHG/KDPG aldolase	0.015
8.3	*lytB*	plu0594	penicillin tolerance protein	0.010
5.4	*galM*	plu0577	aldose 1-epimerase	0.001
4.2	*serB*	plu0551	phosphoserine phosphatase	0.005
3.2	*pgpA*	plu3895	phosphatidylglycerophosphatase A	0.004
3.2	*mend*	plu3073	menaquinone biosynthesis protein menD	0.044
2.4	*astB*	plu3107	succinylarginine dihydrolase	0.020
2.3	*cysD*	plu0709	sulfate adenylyltransferase subunit 2	0.044
2.3	*nuoH*	plu3083	NADH dehydrogenase I chain H (NADH-ubiquinone	0.018
2.3	*Ndh*	plu2821	NADH dehydrogenase	0.016
2.2	*mrsA*	plu4533	Phosphoglucomutase protein MrsA	0.005
2.2	*fumC*	plu2359	fumarate hydratase class II (fumarase)	0.003
2.2	*deoC*	plu0520	2-deoxyribose-5-phosphate aldolase	0.039
2.2	*treC*	plu3287	Trehalose-6-phosphate hydrolase	0.011
2.1	*pula*	plu0105	alpha-dextrin endo-1,6-alpha-glucosidase	0.013
2.1	*pdxA*	plu0610	4-hydroxythreonine-4-phosphate dehydrogenase	0.007
2.1	*trxA*	plu4664	thioredoxin 1 (TRX1) (TRX)	0.034
2.1	*lipA*	plu2191	lipoic acid synthase (LIP-SYN)	0.026
2	*Pta*	plu3096	Phosphate acetyltransferase	0.014
2	*ubiE*	plu4413	ubiquinone/menaquinone biosynthesis	0.002
0.5	*metB*	plu4756	cystathionine gamma-synthase (CGS)	0.013
0.49	*pdxJ*	plu3337	Pyridoxal phosphate biosynthetic protein PdxJ	0.045
0.48	*astD*	plu3108	succinylglutamic semialdehyde dehydrogenase	0.001
0.47	*trpA*	plu2467	tryptophan synthase alpha subunit	0.033
0.47	*cob*	plu2811	CobB protein	0.023
0.47	*ppsA*	plu2628	phosphoenolpyruvate synthase (PEP synthase)	0.029
0.46	*aroQ*	plu4073	3-dehydroquinate dehydratase (3-dehydroquinase)	0.025
0.44	*trpB*	plu2466	tryptophan synthase beta chain	0.028
0.43	*menA*	plu4764	1,4-dihydroxy-2-naphthoate octaprenyltransferas	0.001
0.43	*xylB*	plu1959	xylulose kinase	0.020
0.42	*entB*	plu2728	isochorismatase	0.031
0.38	*moaC*	plu1500	molybdenum cofactor biosynthesis protein C	0.017
0.37	*guaB*	plu2713	inosine-5'-monophosphate dehydrogenase (IMP	0.046
0.37	*Pgk*	plu0956	phosphoglycerate kinase	0.044

0.34	*uxaC*	plu0176	uronate isomerase (glucuronate isomerase)	0.013
0.33	*luxB*	plu2082	Alkanal monooxygenase beta chain (luciferase)	0.003
0.32	*bioB*	plu1485	biotin synthetase (biotin synthase)	0.028
0.32	*celC*	plu2756	PTS system, cellobiose-specific IIA component	0.039
0.32	*celB*	plu2755	PTS system, cellobiose-specific IIC component	0.014
0.3	*eutC*	plu2971	Ethanolamine ammonia-lyase light chain	0.034
0.22	*glpQ*	plu4120	glycerophosphoryl diester phosphodiesterase	0.042
0.22	*aroB*	plu0089	3-dehydroquinate synthase	0.050
0.21	*asnA*	plu0052	Aspartate--ammonia ligase (Asparagine synthetase)	0.053
0.19	*adiA*	plu3319	Biodegradative arginine decarboxylase	0.047
0.17	*hcaF*	plu2205	3-phenylpropionate dioxygenase beta subunit	0.005
0.16	*nqrF*	plu1201	Na+-translocating NADH-ubiquinone	0.018
0.14	*hcaB*	plu2207	2,3-dihydroxy-2,3-dihydrophenylpropionate	0.029
0.12	*fabD*	plu2834	malonyl CoA-acyl carrier protein transacylase	0.002
0.11	*aldB*	plu3739	Aldehyde dehydrogenase B (Lactaldehyde)	0.022
0.065	*hcaE*	plu2204	3-phenylpropionate dioxygenase alpha subunit	0.005
0.051	*glnE*	plu3969	glutamate-ammonia-ligase adenylyltransferase	0.023
0.023	*hcaC*	plu2206	3-phenylpropionate dioxygenase ferredoxin	0.013
Cell structure				
12.4	*murA*	plu4028	UDP-N-acetylglucosamine	0.003
3.7	*ftsI*	plu3660	peptidoglycan synthetase ftsI precursor	0.007
3.3	*Wzt*	plu4817	Wzy protein	0.045
3.3	*mine*	plu2136	Cell division topological specificity factor	0.025
3	*dbhA*	plu0492	NA-binding protein HU-alpha (NS2) (HU-2)	0.052
2.8	*walO*	plu4861	WalO protein	0.219
2.5	*dapE*	plu2722	Succinyl-diaminopimelate desuccinylase (SDAP)	0.024
2.5	*prtC*	plu0658	Membrane Fusion Protein PrtC	0.001
2.4	*rffG*	plu4658	dTDP-glucose 4,6-dehydratase Synthesis of enterobacterial common antigen	0.001
2.1	*wblS*	plu4818	WblS protein	0.035
0.39	*phfC*	plu0996	Unknown, putative fimbrial chaperone	0.007
0.38	*fabA*	plu1772	D-3-hydroxydecanoyl-(acyl carrier-protein)	0.049
0.37	*flgE*	plu1918	Flagellar hook protein FlgE	0.037
0.29	*wblK*	plu4807	WblK protein	0.027
0.27	*wblA*	plu4796	WblA protein	0.047
Regulation				
6.3	*kdpE*	plu1416	transcriptional regulatory protein of kdp	0.007
4.4	*hexA*	plu3090	Transcriptional regulator LrhA (HexA)	0.011
4.3	*clpP*	plu3869	ATP-dependent proteolytic subunit of clpA-clpP	0.002

4.2	*madJ*	plu0270	DUF1401, GrlA/CaiF-like transcriptional activator	0.036
3.2		plu3730	Unknown, probable transcriptional regulator	0.031
2.9	*relB*	plu0254	Negative regulator of translation RelB protein	0.044
2.7	*gcvR*	plu2747	Glycine cleavage system transcriptional	0.004
2.4	*era*	plu3339	GTP-binding protein era	0.025
2.3	*hglK*	plu4579	protease specific for phage lambda cII	0.005
2.3	*surA*	plu0611	Survival protein SurA precursor	0.034
0.48	*rpoS*	plu0719	RNA polymerase sigma factor (sigma-38)	0.005
0.47	*pdhR*	plu3624	pyruvate dehydrogenase complex repressor	0.003
0.46	*uspB*	plu0120	universal stress protein B	0.002
0.45	*csrA*	plu1251	carbon storage regulator homolog	0.013
0.42	*infC*	plu2668	translation initiation factor IF-3	0.025
0.38	*hslJ*	plu2144	Heat shock protein HslJ	0.036
0.32	*htpX*	plu2681	protease HtpX (heat shock protein)	0.003
0.32	*rtcB*	plu4307	Protein RtcB	0.030
0.31	*rmf*	plu1769	ribosome modulation factor (protein E)	0.051
0.29	*ampE*	plu3636	Signaling protein AmpE	0.020
0.2	*rnd*	plu2135	Ribonuclease D (RNase D)	0.032
0.17	-	plu0918	Unknown, probable transcriptional regulator	0.032
0.17	*cspD*	plu1592	cold shock protein	0.019
0.15	*cspC*	plu2783	cold shock protein	0.002
0.088	*cpxP*	plu4793	periplasmic protein precursor	0.023
0.025	*cspE*	plu1289	cold shock-like protein	0.027

Table S3. Strains and plasmids used in the study.

Strains	Description	Reference / Source
Nematode		
Heterorhabditis bacteriophora strain TT01 M31e	Nematode host for *P. luminescens* ssp. *laumondii* TTO1, inbred for 13 generations	Ciche and Sternberg, Caltech
Photorhabdus		
P. luminescens ssp. *laumondii strain* TTO1	Nematode symbiont	Nematode host
P. luminescens ssp. *laumondii* strain TTO1-GFP	Tn7-GFP labeled TTO1	(*10*)
P. temperata NC1	Symbiont of *H. bacteriophora* NC1, colonizes M31e nematodes normally	Nematode host
P. temperata NC1-GFP	Tn7-GFP labeled NC1	(*10*)
P. temperata NC1-dsRed	Tn7-dsRed labeled NC1	(*10*)
TRN16	Transmission defective HimarGm mutant of NC1	(*10*)
Δ*madA::Gm*^{R}	TTO1 containing a mutant *madA* allele fused to FRT-Gm^R-FRT cassette	This study
Δ*madA*	TTO1 containing an unmarked nonpolar *madA* deletion	This study
Δ*madA*-GFP	Δ*madA* labeled with Tn7GFP	This study
Δ*madH::Gm*^{R}	TTO1 containing a mutant *madH* allele fused to FRT-Gm^R-FRT cassette	This study
Δ*madH*	TTO1 containing an unmarked nonpolar *madH* deletion	This study
Δ*madH*-GFP	Δ*madH* labeled with Tn7GFP	This study
Δ*madJ::Gm*^{R}	TTO1 containing a mutant *madJ* allele fused to FRT-Gm^R-FRT cassette	This study
Δ*madJ*	TTO1 containing an unmarked nonpolar *madJ* deletion	This study
Δ*madJ*-GFP	Δ*madJ* labeled with Tn7GFP	This study
Δ*madR::Gm*^{R}	TTO1 containing a mutant *madR* allele fused to FRT-Gm^R-FRT cassette	This study
Δ*madR::Gm*^{R}-GFP	Δ*madR::Gm*^{R} labeled with Tn7GFP	This study
Δ*madO::Gm*^{R}	TTO1 containing a mutant *madO* allele fused to FRT-Gm^R-FRT cassette	This study
Δ*madO::Gm*^{R}-GFP	Δ*madO::Gm*^{R} labeled with Tn7GFP	This study
madswitch-GFP	Unmarked and in-frame promoterless GFP reporter inserted on TTO1 chromosome downstream of *madA*	This study
L/P-form	TTO1 *madswitch* locked in OFF orientation resulting in a locked P-form	This study
L/M-form	TTO1 *madswitch* locked in ON orientation resulting in a locked M-form	This study

E. coli		
E. coli DH5 alpha	Strain for cloning and DNA maintenance	Lab strain collection
E. coli BW29427	*dap* auxotroph, *tra, pir*	K. A. Datsenko and B. L. Wanner, Purdue University
.*E. coli* EC100 *pir-116*	R6Kγ *ori* cloning strain	Epicenter Biotechnologies
Plasmids		
pPS856	Gm^R flanked by Flp recombinase target (FRT) sites	(*33*)
pCP20	Flp recombinase under control of bacteriophage λ rightward promoter,ts λ cI857, ts ori, Cm^R , Ap^R	*E. coli* Genetic Stock Center, Yale University, CT
pSIM5	Plasmid expressing Red recombinase driven by bacteriophage λ P_L , under control of temperature sensitive cI857 λ repressor, pSC101 ori $repA^{ts}$, Cm^R	(*34*)
pFLP2	Flp recombinase driven by rightward λ promoter, regulated by the Ts, *cI*857-encoded λ repressor, Flp fused to the λ Cro ATG initiation codon, Ap^R	(*36*)
pURR25	Source of GFPmut* ORF, $Tn7P_{A1/03/04}$*gfpmut3**	D. Lies / D. Newman, Caltech

Table S4. Oligonucleotides used in the study

Primer	Sequence (5' to 3')	Description
madR-5'Up	aaggcgtgtctggtcttcat	Protein length 188 aa
madR-5'Dn-Gm	tcagagcgcttttgaagctaattcgaacacgaaagccgtggat	Deleted amino acids 43-147
madR-3'Up-Gm	aggaacttcaagatccccaattcgagggatagatacccgact	
madR-3'Dn	gtatccaccgtcccatttga	
madR-Indel-R	cgttgccctaactggttgat	
madA-5'-Up	ttttgctcttgcagatcgag	Protein length 201 aa
madA-5'-Up-Gm	tcagagcgcttttgaagctaattcgcccatttgagccagggttagta	Deleted amino acids 51-147
madA-3'-Dn-Gm	aggaacttcaagatccccaattcgggttgctatgatcgttcctaatg	
madA-3'-Dn	cgcaatcttgtcaccttcaa	
madA-Indel-F	tgttaccggttcgattgtga	
madA-Indel-R	tccctccaaggtgttacctg	
madH-5'Up	tggcaagatgaaaatggtga	Protein length 876 aa
madH-5'Dn-Gm	tcagagcgcttttgaagctaattcgctgacctcctacggtctca	Deleted amino acids 55-863
madH-3'Up-Gm	aggaacttcaagatccccaattcgacgctggaatccaatgag	
madH-3'Dn	acgagcgctactggtgattt	
madH-Indel-R	gctggtatgccgctgatatt	
madJ-5'-Up	gacgcgatattcccaaaaga	Protein length 166 aa,
madJ-5'-Dn-Gm	tcagagcgcttttgaagctaattcgctgacctccaggcaaatc	Deleted amino acids 25-152
madJ-3'-Up-Gm	aggaacttcaagatccccaattcggcgcacttggtttttgca	
madJ-3'-Dn	aaatttatggccgtcgagtg	
madJ-Indel-R	gatcacatcacgtcgctcat	
madO-5'-Up	gccggtttcttctagcaaag	Protein length 206
madO-5'-Dn-Gm	tcagagcgcttttgaagctaattcgcgccacttccagcattctttc	Deleted amino acids 19-195
madO-3'-Up-Gm	aggaacttcaagatccccaattcgcgtcccaaatgaaaatcctt	
madO-3'-Dn	caacatgccgtcaacatagg	
Fim-reporter-5'madA-Up	aacgtgatgcacgagtttga	A promoterless GFP added downstream of *madA* and upstream of *madB* in-frame and markerless by Recombineering to report turning ON of *mad* fimbrial operon
Fim-reporter-5'madA-Dn	gtgaaattgttatccgctcacatcctcaggctaaagccacat	
Fim-reporter-GFP-Up	tgtgagcggataacaatttcac	
Fim-reporter-GFP-Dn	tcagagcgcttttgaagctaattcgttatttgtatagttcatccatgccatgtgtaatc	
Fim-reporter-3'madB-Up	aggaacttcaagatccccaattcggcatctcctcgggcttcttc	
Fim-reporter-3'madB-Dn	aggtgccaacatttgtggat	
Lock-5'Up	gttgtcgggtaaatcggtgt	*Madswitch* locked in ON or OFF orientation by recombination of *madswitch* promoter in either ON or OFF orientation, deleting inverse repeat left and *madR*
Lock-5'Dn-Gm	tcagagcgcttttgaagctaattcgtttcacctcacaagcacgtt	
LockP-3'Up-Gm	aggaacttcaagatccccaattcgaaacgcaactatcctaccac	
Lock-3'Dn	ctttgttaaagagataaccc	
LockM-3'Up-Gm	aggaacttcaagatccccaattcggtgatgtttttacatattgg	

Gm-F	cgaattagcttcaaaagcgctctga	FRT-Gm-FRT cassette
Gm-R	cgaattggggatcttgaagttcct	
Bet F	ggctgacgttctgcagtgta	*bet* Red recombinase genes, confirmation primers
Bet R	acggcatttaaaggtgatgc	
Udp qF	gtgttgtgagccgtttcaag	qPCR internal RNA control
Udp qR	ataacaccggcaaccatacc	
madA qF	acggttgctatgatcgttcc	qPCR for *madA*
madA qR	agcatctgtgctctttgtgg	
madK qF	tgatgtttggtgtgggtgag	qPCR for *madK*
madK qR	cgtcatcccggttatcaaag	
recA qF	atctgtgatgcgttgactcg	qPCR internal RNA control
recA qR	tacgcattgcctgactcatc	
RACE_*madA*	ctgaagagcagtcagcaagaccaa	
RACE_nested_*madA*	gtcccatttgagccagggttagta	

References and Notes

1. E. R. Moxon, P. B. Rainey, M. A. Nowak, R. E. Lenski, Adaptive evolution of highly mutable loci in pathogenic bacteria. *Curr. Biol.* **4**, 24 (1994).

2. N. Q. Balaban, J. Merrin, R. Chait, L. Kowalik, S. Leibler, Bacterial persistence as a phenotypic switch. *Science* **305**, 1622 (2004).

3. T. A. Ciche, J. C. Ensign, For the insect pathogen *Photorhabdus luminescens*, which end of a nematode is out? *Appl. Environ. Microbiol.* **69**, 1890 (2003).

4. N. R. Waterfield, T. Ciche, D. Clarke, *Photorhabdus* and a host of hosts. *Annu. Rev. Microbiol.* **63**, 557 (2009).

5. D. J. Bowen, J. C. Ensign, Purification and characterization of a high-molecular-weight insecticidal protein complex produced by the entomopathogenic bacterium *Photorhabdus luminescens*. *Appl. Environ. Microbiol.* **64**, 3029 (1998).

6. D. Bowen *et al*., Insecticidal toxins from the bacterium *Photorhabdus luminescens*. *Science* **280**, 2129 (1998).

7. P. J. Daborn *et al*., A single *Photorhabdus* gene, *makes caterpillars floppy* (*mcf*), allows *Escherichia coli* to persist within and kill insects. *Proc. Natl. Acad. Sci. U.S.A.* **99**, 10742 (2002).

8. S. B. Bintrim, J. C. Ensign, Insertional inactivation of genes encoding the crystalline inclusion proteins of *Photorhabdus luminescens* results in mutants with pleiotropic phenotypes. *J. Bacteriol.* **180**, 1261 (1998).

9. W. H. Richardson, T. M. Schmidt, K. H. Nealson, Identification of an anthraquinone pigment and a hydroxystilbene antibiotic from *Xenorhabdus luminescens*. *Appl. Environ. Microbiol.* **54**, 1602 (1988).

10. T. A. Ciche, K. S. Kim, B. Kaufmann-Daszczuk, K. C. Nguyen, D. H. Hall, Cell invasion and matricide during *Photorhabdus luminescens* transmission by *Heterorhabditis bacteriophora* nematodes. *Appl. Environ. Microbiol.* **74**, 2275 (2008).

11. V. S. Somvanshi, B. Kaufmann-Daszczuk, K. S. Kim, S. Mallon, T. A. Ciche, *Mol. Microbiol.* **77**, 1021 (2010).

12. S. P. Nuccio, A. J. Bäumler, Evolution of the chaperone/usher assembly pathway: Fimbrial classification goes Greek. *Microbiol. Mol. Biol. Rev.* **71**, 551 (2007).

13. R. E. Hurlbert, J. Xu, C. L. Small, Colonial and cellular polymorphism in *Xenorhabdus luminescens*. *Appl. Environ. Microbiol.* **55**, 1136 (1989).

14. R. J. Akhurst, Morphological and functional dimorphism in *Xenorhabdus* spp., bacteria symbiotically associated with the insect pathogenic nematodes *Neoaplectana* and *Heterorhabditis. J. Gen. Microbiol.* **121**, 303 (1980).

15. J. Zieg, M. Hilmen, M. Simon, Regulation of gene expression by site-specific inversion. *Cell* **15**, 237 (1978).

16. M. W. van der Woude, A. J. Bäumler, Phase and antigenic variation in bacteria. *Clin. Microbiol. Rev.* **17**, 581 (2004).

17. K. Eichler, A. Buchet, R. Lemke, H. P. Kleber, M. A. Mandrand-Berthelot, Identification and characterization of the caiF gene encoding a potential transcriptional activator of carnitine metabolism in Escherichia coli. *J. Bacteriol.* **178**, 1248 (1996).

18. W. Deng *et al*., Dissecting virulence: Systematic and functional analyses of a pathogenicity island. *Proc. Natl. Acad. Sci. U.S.A.* **101**, 3597 (2004).

19. J. M. Crawford, R. Kontnik, J. Clardy, Regulating alternative lifestyles in entomopathogenic bacteria. *Curr. Biol.* **20**, 69 (2010).

20. S. A. Joyce *et al*., Bacterial biosynthesis of a multipotent stilbene. *Angew. Chem. Int. Ed. Engl.* **47**, 1942 (2008).

21. I. Eleftherianos *et al*., An antibiotic produced by an insect-pathogenic bacterium suppresses host defenses through phenoloxidase inhibition. *Proc. Natl. Acad. Sci. U.S.A.* **104**, 2419 (2007).

22. J. S. Williams, M. Thomas, D. J. Clarke, The gene *stlA* encodes a phenylalanine ammonia-lyase that is involved in the production of a stilbene antibiotic in *Photorhabdus luminescens* TT01. *Microbiology* **151**, 2543 (2005).

23. S. Chalabaev *et al*., Cinnamic acid, an autoinducer of its own biosynthesis, is processed via Hca enzymes in *Photorhabdus luminescens*. *Appl. Environ. Microbiol.* **74**, 1717 (2008).

24. R. A. Proctor *et al*., Small colony variants: A pathogenic form of bacteria that facilitates persistent and recurrent infections. *Nat. Rev. Microbiol.* **4**, 295 (2006).

25. K. Lewis, Persister cells. *Annu. Rev. Microbiol.* **64**, 357 (2010).

26. K. S. Makarova *et al*., Evolution and classification of the CRISPR-Cas systems. *Nat. Rev. Microbiol.* **9**, 467 (2011).

27. S. A. Joyce, D. J. Clarke, A *hexA* homologue from *Photorhabdus* regulates pathogenicity, symbiosis and phenotypic variation. *Mol. Microbiol.* **47**, 1445 (2003).

28. D. J. Bowen *et al*., Genetic and biochemical characterization of PrtA, an RTX-like metalloprotease from *Photorhabdus*. *Microbiology* **149**, 1581 (2003).

29. M. Acar, J. T. Mettetal, A. van Oudenaarden, Stochastic switching as a survival strategy in fluctuating environments. *Nat. Genet.* **40**, 471 (2008).

30. R. Edgar, M. Domrachev, A. E. Lash, Gene Expression Omnibus: NCBI gene expression and hybridization array data repository. *Nucleic Acids Res.* **30**, 207 (2002).

31. J. Sambrook, E. F. Fritsch, T. Maniatis, *Molecular Cloning : A Laboratory Manual* (Cold Spring Harbor Laboratory Press, Cold Spring Harbor, NY, 1989).

32. N. G. Copeland, N. A. Jenkins, D. L. Court, Recombineering: A powerful new tool for mouse functional genomics. *Nat. Rev. Genet.* **2**, 769 (2001).

33. K. H. Choi, H. P. Schweizer, An improved method for rapid generation of unmarked *Pseudomonas aeruginosa* deletion mutants. *BMC Microbiol.* **5**, 30 (2005).

34. S. Datta, N. Costantino, D. L. Court, A set of recombineering plasmids for gram-negative bacteria. *Gene* **379**, 109 (2006).

35. P. P. Cherepanov, W. Wackernagel, Gene disruption in *Escherichia coli*: Tc^R and Km^R cassettes with the option of Flp-catalyzed excision of the antibiotic-resistance determinant. *Gene* **158**, 9 (1995).

36. T. T. Hoang, R. R. Karkhoff-Schweizer, A. J. Kutchma, H. P. Schweizer, A broad-host-range Flp-FRT recombination system for site-specific excision of chromosomally-located DNA sequences: Application for isolation of unmarked *Pseudomonas aeruginosa* mutants. *Gene* **212**, 77 (1998).

37. J. Liu, F. B. Dazzo, O. Glagoleva, B. Yu, A. K. Jain, CMEIAS: A computer-aided system for the image analysis of bacterial morphotypes in microbial communities. *Microb. Ecol.* **41**, 173 (2001).

38. C. D. Wilcox, W. Doss-McDavid, D. B. Greer, UTHSCSA ImageTool Version 1.27 (Univ. Texas Health Science Center, San Antonio, TX, 1997); http://compdent.uthscsa.edu/dig/itdesc.html.

39. B. Schwyn, J. B. Neilands, Universal chemical assay for the detection and determination of siderophores. *Anal. Biochem.* **160**, 47 (1987).

40. A. Givaudan, S. Baghdiguian, A. Lanois, N. Boemare, Swarming and swimming changes concomitant with phase variation in *Xenorhabdus nematophilus*. *Appl. Environ. Microbiol.* **61**, 1408 (1995).

41. G. A. O'Toole, R. Kolter, Initiation of biofilm formation in *Pseudomonas fluorescens* WCS365 proceeds via multiple, convergent signalling pathways: A genetic analysis. *Mol. Microbiol.* **28**, 449 (1998).

42. B. A. Bensing, B. J. Meyer, G. M. Dunny, Sensitive detection of bacterial transcription initiation sites and differentiation from RNA processing sites in the pheromone-induced plasmid transfer system of Enterococcus faecalis. *Proc. Natl. Acad. Sci. U.S.A.* **93**, 7794 (1996).